ARL-TR-95-19

Copy No. 68

Nonlinear Properties of In-Situ Sediment Gas Bubbles

Final Report under Subcontract 449382,
Applied Physics Laboratory, The University of Washington

Frank A. Boyle
Nicholas P. Chotiros

Applied Research Laboratories
The University of Texas at Austin
P. O. Box 8029 Austin, TX 78713-8029

21 July 1995

Final Report

1 October 1994 - 31 May 1995

Approved for public release;
distribution is unlimited.

Prepared for:

Applied Physics Laboratory
The University of Washington
1013 NE 40th Street
Seattle, WA 98105-6698

DISCLAIMER NOTICE

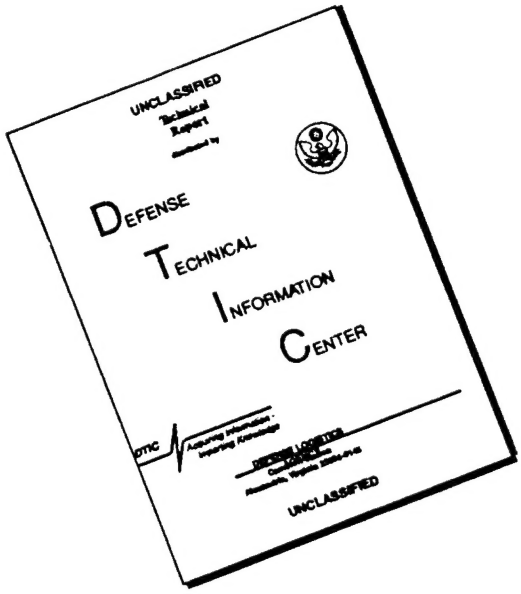

THIS DOCUMENT IS BEST QUALITY AVAILABLE. THE COPY FURNISHED TO DTIC CONTAINED A SIGNIFICANT NUMBER OF PAGES WHICH DO NOT REPRODUCE LEGIBLY.

REPORT DOCUMENTATION PAGE

Form Approved
OMB No. 0704-0188

1. AGENCY USE ONLY (Leave blank)	2. REPORT DATE	3. REPORT TYPE AND DATES COVERED
	21 Jul 95	final 1 Oct 94 - 31 May 95

4. TITLE AND SUBTITLE

Nonlinear Properties of In-Situ Sediment Gas Bubbles, Final Report under Subcontract 449382, Applied Physics Laboratory, The University of Washington

5. FUNDING NUMBERS

Subcontract 449382

6. AUTHOR(S)

Boyle, Frank A. Chotiros, Nicholas P.

7. PERFORMING ORGANIZATION NAMES(S) AND ADDRESS(ES)

Applied Research Laboratories
The University of Texas at Austin
P.O. Box 8029
Austin, Texas 78713-8029

8. PERFORMING ORGANIZATION REPORT NUMBER

ARL-TR-95-19

9. SPONSORING/MONITORING AGENCY NAME(S) AND ADDRESS(ES)

Applied Physics Laboratory
The University of Washington
1013 NE 40th Street
Seattle, WA 98105-6698

10. SPONSORING/MONITORING AGENCY REPORT NUMBER

11. SUPPLEMENTARY NOTES

12a. DISTRIBUTION/AVAILABILITY STATEMENT

Distribution approved for public release; distribution is unlimited.

12b. DISTRIBUTION CODE

13. ABSTRACT (Maximum 200 words)

A model for difference frequency backscatter from trapped bubbles in sandy sediments is developed. A nonlinear volume scattering coefficient is computed via a technique similar to that of Ostrovsky and Sutin ["Nonlinear sound scattering from subsurface bubble layers", in Natural Physical Sources of Underwater Sound, B. R. Kerman (ed.), 363-373 (1993)] which treats the case of bubbles surrounded by water. The Biot theory is incorporated to model the acoustics of sandy sediment. Biot fast and slow waves are included by modeling the pore fluid as a superposition of two acoustic fluids with effective densities that differ from the pore fluid's actual density and account for its confinement within sediment pores. The principle of acoustic reciprocity is employed to develop an expression for the backscattering strength.

14. SUBJECT TERMS

acoustic scattering, backscatter, Biot, bubble resonance, difference frequency, gassy sediment, nonlinear, parametric, poroelastic, microbubble, sediment

15. NUMBER OF PAGES

53

16. PRICE CODE

17. SECURITY CLASSIFICATION OF REPORT	18. SECURITY CLASSIFICATION OF THIS PAGE	19. SECURITY CLASSIFICATION OF ABSTRACT	20. LIMITATION OF ABSTRACT
UNCLASSIFIED	UNCLASSIFIED	UNCLASSIFIED	SAR

NSN 7540-01-280-5500

Standard Form 298 (Rev. 2-89)
Prescribed by ANSI Std. 239-18
298-102

TABLE OF CONTENTS

This page intentionally left blank.

LIST OF FIGURES

This page intentionally left blank.

PREFACE

This report is the final report on the work ARL:UT completed under Subcontract 449382 for Applied Physics Laboratory, The University of Washington.

I. INTRODUCTION

Acoustic scattering from the ocean floor has been an item of considerable interest in recent years. Since there is no general agreement on what the basic scattering mechanisms are, a lot of models have been developed, based on several different scattering mechanisms. Some models[1,2] assume that the scattering occurs at the fluid/sediment interface. Other models[3-7] consider scattering from within the sediment volume below the interface. Volume scatterers that have been considered include variations in the refractive index of the sediment caused by local variations of the sound speed or density, the sediment grains, fluid pockets between grains and, most recently, trapped gas bubbles. It is reasonable that, when gas is present in sufficient quantity, the gas bubble scattering might dominate, since gas bubbles in resonance are very strong scatterers of sound, with scattering cross sections that are typically 1000 times their geometric cross section.[8] The model of Boyle and Chotiros[9] suggests that very small amounts of gas (fluid gas fractions of 10^{-5} or less) are sufficient to dominate the other scattering mechanisms.

A resulting difficulty in modeling acoustic backscatter is that the backscattering strength of a gassy sediment depends sensitively on the fluid gas fraction. There is at present no practical method of measuring, in situ, small amounts of gas.

Actual sediments may contain more than one type of scatterer, with acoustic returns that appear quite similar. For example, a hard rock surface may look very much like a pocket of trapped gas. This problem might seriously affect any attempt at remote acoustic classification of sediment. Therefore finding a way of distinguishing gas bubble acoustic returns from other types is critical.

One way in which gas bubbles differ from other kinds of scatterers is in their nonlinear scattering properties. Water has a nonlinearity parameter B/A of about 5-6 compared with a value of 8-12 for water saturated sand.[10] The value for the gas inside a bubble is much higher.[11]

One possible way of identifying bubble returns would be to insonify the sediment with a parametric signal and measure the scattered sound at the

difference frequency. This procedure has been successfully employed to detect bubbles in the water column.[12]

The problem of identifying gas bubbles trapped within sediment pores is considerably more complicated than identifying bubbles in the water column. Recent experiments[13,14] suggest that sandy sediments, which are common in coastal areas, are best modeled acoustically via Biot's[15,16] poroelastic theory. This type of treatment differs from others in that it models a saturated sediment as a two-phase medium, consisting of a semi-rigid structure of sediment grains through which the pore fluid is allowed to flow. An outstanding feature of Biot's theory is that two compressional waves are predicted, in addition to the shear wave. In the so-called Biot fast wave, the pore fluid and grain structure move approximately in phase. This wave is analogous to the compressional wave that would exist in an equivalent elastic medium. The other type of compressional wave, called the Biot slow wave, consists of the solid and fluid parts of the medium moving out of phase. The experiments suggest that both types of waves can be significant. For trapped bubble scattering calculations, shear waves can be neglected since they couple only weakly into the pore fluid that contains the scattering bubbles.

As a bubble expands, it pushes against the surrounding pore fluid. Partial confinement within sediment pores will cause the fluid to behave as if it had an effective density different from its actual density. Since the mechanics of fluid confinement are different for Biot fast and slow waves, the pore fluid can be expected to have two different effective densities, depending on whether fast or slow waves are propagating. Similarly, the fluid acoustic impedance and the bubble's resonance frequency and damping constant are specific for each of the Biot waves. Furthermore, whereas for a fluid model these quantities can generally be treated as constants, in the Biot case they are functions of frequency.

In this report, an expression for the difference frequency scattering cross section from a bubbly sediment is developed. It separately models scattering from Biot fast waves and Biot slow waves by modeling the medium as a superposition of two acoustic fluids. One fluid supports the fast wave while the other supports the slow wave. This is attained by assigning an appropriate

effective density and acoustic impedance to each fluid. The densities and impedances are obtained from the Biot model of Stern, Bedford, and Millwater.[17] Shear waves are neglected since they exist primarily in the solid part of the medium and do not couple strongly into the pore fluid that contains the scattering bubbles.

In Section 2, an expression for the difference frequency scattering cross section from a single bubble in an acoustic fluid is derived. The bubble's resonance frequency and damping constant, as well as the surrounding fluid's density and acoustic impedance, are allowed to vary with frequency. In Section 3 the scattering cross section from a distribution of bubble sizes is computed. Section 4 contains a calculation of the effective backscattering strength of the interface above a bubbly Biot medium. Conclusions are discussed in Section 5.

This page intentionally left blank.

2. CALCULATION OF THE DIFFERENCE FREQUENCY SCATTERING CROSS SECTION FROM A SINGLE BUBBLE

Ostrovsky and Sutin[18] developed an expression for the difference frequency scattering cross section from bubbles in an acoustic fluid. The following development follows their technique, allowing for the frequency dependence of the pore fluid's effective density and acoustic impedance and the bubble's damping constant and resonance frequency.

In Appendix A, Zabolotskaya and Soluyan's[19] equation of motion for a bubble's surface is derived:

$$\ddot{V} + \omega_0^2 V - \alpha V^2 - \beta\left(2\ddot{V}V + \dot{V}^2\right) + \omega\delta\dot{V} = -\varepsilon P \ , \qquad (2.1)$$

where V is a perturbation in the bubble's volume, P is the acoustic pressure incident upon the bubble, ω is the frequency of volume oscillations, and ω_0, α, β, δ, and ε are real quantities that are allowed to vary with frequency. The bubble's radius is assumed small in comparison with the acoustic wavelength. A solution is needed, given a bi-harmonic acoustic pressure incident upon the bubble:

$$P = P_1\cos(\omega_1 t + \varphi_1) + P_2\cos(\omega_2 t + \varphi_2) \ , \qquad (2.2)$$

where P_1 and P_2 are amplitudes and φ_1 and φ_2 are corresponding phases of two superimposed incident pressure signals with frequencies ω_1 and ω_2. As an ansatz, let V be of the form

$$V = V_1\cos(\omega_1 t + \xi_1) + V_2\cos(\omega_2 t + \xi_2) + V_\Omega\cos(\Omega t + \xi_\Omega) + \Psi \ , \qquad (2.3)$$

where $\Omega = \omega_1 - \omega_2$ is the difference frequency. V_i and ξ_i are amplitudes and phases of superimposed components of V. "Ψ" includes all other terms, including those involving the sum frequency and higher harmonics of the driving frequencies ω_1 and ω_2. To solve for V_1 and V_2, it is only necessary to consider the linear part of Eq. (2.1):

$$\ddot{V} + \omega_0^2 V + \omega\delta\dot{V} = -\varepsilon P \quad , \tag{2.4}$$

where ω_0, δ, and ε are functions of the frequency ω of V. The linear part of V is given by

$$V_{lin} = V_1\cos(\omega_1 t + \xi_1) + V_2\cos(\omega_2 t + \xi_2) \; . \tag{2.5}$$

Upon substituting Eqs. (2.5) and (2.2) into Eq. (2.4),

$$\begin{bmatrix} (\omega_{01}^2 - \omega_1^2)V_1\cos(\omega_1 t + \xi_1) + \delta_1\omega_1^2 V_1\sin(\omega_1 t + \xi_1) \\ +(\omega_{02}^2 - \omega_2^2)V_2\cos(\omega_2 t + \xi_2) + \delta_2\omega_2^2 V_2\sin(\omega_2 t + \xi_2) \end{bmatrix} = \begin{bmatrix} -\varepsilon_1 P_1\cos(\omega_1 t + \varphi_1) \\ -\varepsilon_2 P_2\cos(\omega_2 t + \varphi_2) \end{bmatrix} \; . \tag{2.6}$$

If Eq. (2.6) is valid for all possible values of time t, the ω_1 and ω_2 components must satisfy it separately. Hence,

$$(\omega_{01}^2 - \omega_1^2)V_1\cos(\omega_1 t + \xi_1) + \delta_1\omega_1^2 V_1\sin(\omega_1 t + \xi_1) = -\varepsilon_1 P_1\cos(\omega_1 t + \varphi_1) \tag{2.7}$$

$$(\omega_{02}^2 - \omega_2^2)V_2\cos(\omega_2 t + \xi_2) + \delta_2\omega_2^2 V_2\sin(\omega_2 t + \xi_2) = -\varepsilon_2 P_2\cos(\omega_2 t + \varphi_2) \; . \tag{2.8}$$

By equating magnitudes on either side of Eqs. (2.7) and (2.8), the amplitudes V_1 and V_2 are obtained:

$$V_1 = \frac{\varepsilon_1 P_1}{\sqrt{(\omega_{01}^2 - \omega_1^2)^2 + \delta_1^2\omega_1^4}} \tag{2.9}$$

$$V_2 = \frac{\varepsilon_2 P_2}{\sqrt{(\omega_{02}^2 - \omega_2^2)^2 + \delta_2^2\omega_2^4}} \; . \tag{2.10}$$

In order to find the difference frequency component V_Ω of the bubble volume perturbation V, it is necessary to consider the complete nonlinear equation, Eq. (2.1). Each term in this equation will have a contribution to V_Ω. The first nonlinear term in Eq. (2.1) is $(-\alpha V^2)$. To find the $(\omega_1-\omega_2)$ component of V^2, apply expression (2.3):

$$V^2 = V_1{}^2\cos^2\left(\omega_1 t + \xi_1\right) + 2V_1V_2\cos\left(\omega_1 t + \xi_1\right)\cos\left(\omega_2 t + \xi_2\right) + V_2{}^2\cos^2\left(\omega_2 t + \xi_2\right) + \text{higher order terms} \tag{2.11}$$

By invoking the trigonometric identity

$$\cos(a)\cos(b) = \frac{1}{2}\left(\cos(a+b) + \cos(a-b)\right), \tag{2.12}$$

the difference frequency component of V^2 can be computed:

$$\left(V^2\right)_\Omega = V_1V_2\cos\left[\Omega t + \left(\xi_1 - \xi_2\right)\right]. \tag{2.13}$$

In similar fashion, the difference frequency components of the other nonlinear terms in Eq. (2.1) can be computed:

$$\left(\ddot{V}V\right)_\Omega = \frac{\left(-\omega_1^2 - \omega_2^2\right)}{2}V_1V_2\cos\left[\Omega t + \left(\xi_1 - \xi_2\right)\right] \tag{2.14}$$

$$\left(\dot{V}^2\right)_\Omega = \omega_1\omega_2V_1V_2\cos\left[\Omega t + \left(\xi_1 - \xi_2\right)\right]. \tag{2.15}$$

The linear terms of Eq. (2.1) also have Ω components:

$$\left(V\right)_\Omega = V_\Omega\cos\left(\Omega t + \xi_3\right) \tag{2.16}$$

$$\left(\dot{V}\right)_\Omega = \Omega V_\Omega\sin\left(\Omega t + \xi_3\right) \tag{2.17}$$

$$\left(\ddot{V}\right)_\Omega = -\Omega^2V_\Omega\cos\left(\Omega t + \xi_3\right). \tag{2.18}$$

The total Ω component of Eq. (2.1) is the sum of contributions from each of its terms. Therefore, by substituting Eqs. (2.13 - 2.18) into Eq. (2.1) and noting that the incident pressure P has no difference frequency component,

$$
\begin{aligned}
&\{-\Omega^2 V_\Omega \cos(\Omega t + \xi_3) \\
&+ \omega_{0\Omega}{}^2 V_\Omega \cos(\Omega t + \xi_3) \\
&- \alpha_\Omega V_1 V_2 \cos\left[\Omega t + (\xi_1 - \xi_2)\right] \\
&- \beta_\Omega \left(-\omega_1^2 - \omega_2^2\right) V_1 V_2 \cos\left[\Omega t + (\xi_1 - \xi_2)\right] \\
&- \beta_\Omega \omega_1 \omega_2 V_1 V_2 \cos\left[\Omega t + (\xi_1 - \xi_2)\right] \\
&+ \delta_\Omega \Omega^2 V_\Omega \sin(\Omega t + \xi_3)\} = 0 \quad , \qquad (2.19)
\end{aligned}
$$

where $\omega_{0\Omega}$, α_Ω, β_Ω, and δ_Ω are the values of ω_0, α, β, and δ at the difference frequency Ω. Rearranging,

$$
\begin{aligned}
&(\omega_{0\Omega}{}^2 - \Omega^2) V_\Omega \cos(\Omega t + \xi_3) + \delta_\Omega \Omega^2 V_\Omega \sin(\Omega t + \xi_3) \\
&= (\alpha_\Omega - \beta_\Omega(\omega_1^2 + \omega_2^2 - \omega_1\omega_2)) V_1 V_2 \cos[\Omega t + (\xi_1 - \xi_2)] \; . \qquad (2.20)
\end{aligned}
$$

Expression (2.20) is an equality of harmonic signals. For two harmonic signals to be equal, their magnitudes and phases must be equal. By equating the magnitudes on either side of Eq. (2.20),

$$
\left| \sqrt{(\omega_{0\Omega}{}^2 - \Omega^2)^2 + \delta_\Omega{}^2 \Omega^4}\, V_\Omega \right| = \left| (\alpha_\Omega - \beta_\Omega(\omega_1^2 + \omega_2^2 - \omega_1\omega_2)) V_1 V_2 \right| \quad ; \qquad (2.21)
$$

hence the amplitude of the difference frequency oscillations of the bubble volume V is

$$
|V_\Omega| = \left| \frac{(\alpha_\Omega - \beta_\Omega(\omega_1^2 + \omega_2^2 - \omega_1\omega_2)) V_1 V_2}{\sqrt{(\omega_{0\Omega}{}^2 - \Omega^2)^2 + \delta_\Omega{}^2 \Omega^4}} \right| \; . \qquad (2.22)
$$

Upon inserting expressions (2.9) and (2.10) for V_1 and V_2,

$$|V_\Omega| = \left| \frac{\left(\alpha_\Omega - \beta_\Omega\left(\omega_1^2+\omega_2^2-\omega_1\omega_2\right)\right)\varepsilon_1\varepsilon_2 P_1 P_2}{\sqrt{\left(\omega_{0\Omega}{}^2-\Omega^2\right)^2+\delta_\Omega{}^2\Omega^4}\sqrt{\left(\omega_{01}{}^2-\omega_1{}^2\right)^2+\delta_1{}^2\omega_1{}^4}\sqrt{\left(\omega_{02}{}^2-\omega_2{}^2\right)^2+\delta_2{}^2\omega_2{}^4}} \right| . \tag{2.23}$$

This expression reduces to that of Zabolotskaya and Sutin[20] for the special case where ω_0, α, β, and δ are independent of frequency.

As the bubble's volume oscillates at frequency Ω, a pressure $P_\Omega(r)$ is generated in the surrounding fluid at distance r from the bubble's center. In Appendix B, an equation is derived that relates this pressure to the bubble's volume perturbation V_Ω:

$$|P_\Omega(r)| = \frac{\Omega^2\rho_\Omega|V_\Omega|}{4\pi r} . \tag{2.24}$$

Upon substituting Eq. (2.23) for $|V_\Omega|$ in Eq. (2.24),

$$|P_\Omega(r)| = \left| \frac{\Omega^2\rho_\Omega\left(\alpha_\Omega - \beta_\Omega\left(\omega_1^2+\omega_2^2-\omega_1\omega_2\right)\right)\varepsilon_1\varepsilon_2 P_1 P_2}{4\pi r\sqrt{\left(\omega_{0\Omega}{}^2-\Omega^2\right)^2+\delta_\Omega{}^2\Omega^4}\sqrt{\left(\omega_{01}{}^2-\omega_1{}^2\right)^2+\delta_1{}^2\omega_1{}^4}\sqrt{\left(\omega_{02}{}^2-\omega_2{}^2\right)^2+\delta_2{}^2\omega_2{}^4}} \right| . \tag{2.25}$$

The scattering cross section of the bubble is the time average of the scattered power divided by the incident intensity:

$$\sigma = 4\pi r^2 \left| \frac{P_\Omega(r)v_\Omega(r)}{P_1 v_1 + P_2 v_2} \right| , \tag{2.26}$$

where P_1 and P_2 are the acoustic pressure amplitudes carried by the incident waves upon the bubble, defined in Eq. (2.2). The quantities v_1 and v_2 are the corresponding fluid velocities. $P_\Omega(r)$ and $v_\Omega(r)$ are the pressure and velocity amplitudes carried by the scattered wave from the bubble at distance r.

In terms of local acoustic impedances $Z_i = dP_i/dv_i$,

$$\sigma = 4\pi r^2 \left| \frac{\left(P_\Omega(r)\right)^2}{P_1^2 \frac{Z_\Omega}{Z_1} + P_2^2 \frac{Z_\Omega}{Z_2}} \right| \quad . \tag{2.27}$$

Substitution of Eq. (2.25) for $P_\Omega(r)$ in Eq. (2.27) yields

$$\sigma = \left| \frac{\Omega^4 \rho_\Omega^2 (\alpha_\Omega - \beta_\Omega(\omega_1^2 + \omega_2^2 - \omega_1\omega_2))^2 \varepsilon_1^2 \varepsilon_2^2 P_1^2 P_2^2}{4\pi\left[(\omega_{0\Omega}^2 - \Omega^2)^2 + \delta_\Omega^2 \Omega^4\right]\left[(\omega_{01}^2 - \omega_1^2)^2 + \delta_1^2 \omega_1^4\right]\left[(\omega_{02}^2 - \omega_2^2)^2 + \delta_2^2 \omega_2^4\right]\left[P_1^2 \frac{Z_\Omega}{Z_1} + P_2^2 \frac{Z_\Omega}{Z_2}\right]} \right| \quad . \tag{2.28}$$

Upon substituting the following expressions, defined in Appendix A,

$$\beta_\Omega = \frac{1}{8\pi R_{eq}^3} \quad , \tag{2.29}$$

$$\varepsilon_1 = \frac{4\pi R_{eq}}{\rho_1} \quad , \tag{2.30}$$

$$\varepsilon_2 = \frac{4\pi R_{eq}}{\rho_2} \quad , \tag{2.31}$$

$$\alpha_\Omega = 3\beta_\Omega(\gamma+1)\omega_{0\Omega}^2 \quad , \tag{2.32}$$

the following expression for the bubble scattering cross section is obtained:

$$\sigma = \left| \frac{\pi\Omega^4 \rho_\Omega^2 (3(\gamma+1)\omega_{0\Omega}^2 - \omega_1^2 - \omega_2^2 + \omega_1\omega_2)^2 P_1^2 P_2^2}{R_{eq}^2 \rho_1^2 \rho_2^2 \left[(\omega_{0\Omega}^2 - \Omega^2)^2 + \delta_\Omega^2 \Omega^4\right]\left[(\omega_{01}^2 - \omega_1^2)^2 + \delta_1^2 \omega_1^4\right]\left[(\omega_{02}^2 - \omega_2^2)^2 + \delta_2^2 \omega_2^4\right]\left[P_1^2 \frac{Z_\Omega}{Z_1} + P_2^2 \frac{Z_\Omega}{Z_2}\right]} \right| \tag{2.33}$$

3. DIFFERENCE FREQUENCY SCATTERING CROSS SECTION FROM A DISTRIBUTION OF BUBBLES IN AN ACOUSTIC FLUID

Of interest is the scattering cross section per unit volume of a sediment that contains trapped bubbles. If we make a single scattering assumption, based on resonance scattering as a dominant effect,[21] we can write the volume scattering cross section in the following form:

$$\beta = \int_0^\infty \sigma n(R_{eq}) dR_{eq} \quad , \tag{3.1}$$

where R_{eq} is the equilibrium bubble radius and $n(R_{eq})$ is the bubble size density function, defined as

$$n(R_{eq}) = \frac{dN(R_{eq})}{dR_{eq}} \quad , \tag{3.2}$$

where $N(R_{eq})$ is the number of bubbles per unit volume with radii less than R_{eq}.

A combination of Eqs. (3.1) and (3.2) results in an integral that is very difficult to solve analytically. A technique originally employed by Wildt[22] yields an approximate expression, based on the following assumptions:

1. Most of the scattering is from bubbles with radii near the resonance radius.

2. The bubble size density function is approximately constant in each range of bubble size that contributes.

3. The damping constant d is approximately constant in each range of bubble size that contributes.

Medwin's[23] expression for the resonance frequency f_0 in terms of the equilibrium bubble radius is

$$f_0 = \frac{\sqrt{\frac{3\gamma b\beta P_{eq}}{\rho}}}{2\pi R_{eq}} \quad , \tag{3.3}$$

where γ is the ratio of specific heats, P_{eq} is the ambient pressure, ρ is the ambient density, and b and β are quantities that account for surface tension and thermal conductivity.

By inversion, the resonance radius R_r is given in terms of applied frequency f:

$$R_0 = \frac{\sqrt{\frac{3\gamma b\beta P_{eq}}{\rho}}}{2\pi f} \quad . \tag{3.4}$$

By combination of Eqs. (3.3) and (3.4),

$$\frac{f_0}{f} = \frac{R_0}{R_{eq}} \quad . \tag{3.5}$$

Therefore,

$$\frac{\omega_{01}}{\omega_1} = \frac{R_{01}}{R_{eq}} \, , \quad \frac{\omega_{02}}{\omega_2} = \frac{R_{02}}{R_{eq}} \, , \quad \frac{\omega_{0\Omega}}{\Omega} = \frac{R_{0\Omega}}{R_{eq}} \quad , \tag{3.6}$$

where R_{01} is the resonance radius of a bubble driven at angular frequency ω_1. By combining Eqs. (3.6) and (2.33),

$$\sigma_\Omega = \frac{\pi\rho_\Omega^2\left[3(\gamma+1)\omega_0^2 - \omega_1^2 - \omega_2^2 - \omega_1\omega_2\right]^2 P_1^2 P_2^2}{\rho_1^2\rho_2^2 R_{eq}^2\omega_1^4\omega_2^4\left[\left(\frac{R_{01}^2}{R_{eq}^2}-1\right)^2 + \delta_1^2\right]\left[\left(\frac{R_{02}^2}{R_{eq}^2}-1\right)^2 + \delta_2^2\right]\left[\left(\frac{R_{0\Omega}^2}{R_{eq}^2}-1\right)^2 + \delta_\Omega^2\right]\left[P_1^2\frac{Z_\Omega}{Z_1} + P_2^2\frac{Z_\Omega}{Z_2}\right]} \, . \tag{3.7}$$

By inspection, it is clear that Eq. (3.7) will have maxima when $R=R_{01}$, $R=R_{02}$, $R=R_{0\Omega}$. The height of these maxima will be determined by the values of the damping constants δ_1, δ_2, and δ_Ω. Assumption (1) is a statement that the

maxima are high enough that most of the contribution to the integral in Eq. (3.1) comes from bubbles with radii very close to R_{01}, R_{02}, or $R_{0\Omega}$.:

$$\beta = \beta_1+\beta_2+\beta_\Omega = \int_{R_{01}-\varepsilon}^{R_{01}+\varepsilon} \sigma n(R_{eq})dR_{eq} + \int_{R_{02}-\varepsilon}^{R_{02}+\varepsilon} \sigma n(R_{eq})dR_{eq} + \int_{R_{0\Omega}-\varepsilon}^{R_{0\Omega}+\varepsilon} \sigma n(R_{eq})dR_{eq} \ . \quad (3.8)$$

Consider β_Ω, which is the contribution from bubbles with radius close to $R_{0\Omega}$.:

$$\beta_\Omega = \int_{R_{0\Omega}-\varepsilon}^{R_{0\Omega}+\varepsilon} \sigma n(R_{eq})dR_{eq}$$

$$= \frac{\rho_\Omega^2 P_1^2 P_2^2}{\rho_1^2\rho_2^2\omega_1^4\omega_2^4\left[P_1^2\frac{Z_\Omega}{Z_1}+P_2^2\frac{Z_\Omega}{Z_2}\right]} \int_{R_{0\Omega}-\varepsilon}^{R_{0\Omega}+\varepsilon} \frac{[3(\gamma+1)\omega_0^2-\omega_1^2-\omega_2^2-\omega_1\omega_2]^2 n(R_{eq})dR_{eq}}{R_{eq}^2\left[\left(\frac{R_{01}^2}{R_{eq}^2}-1\right)^2+\delta_1^2\right]\left[\left(\frac{R_{02}^2}{R_{eq}^2}-1\right)^2+\delta_2^2\right]\left[\left(\frac{R_{0\Omega}^2}{R_{eq}^2}-1\right)^2+\delta_\Omega^2\right]} \ . \quad (3.9)$$

According to assumption (2), the bubble size density function $n(R_{eq})=n(R_{0\Omega})$ is constant within the narrow range of bubble radii about $R_{0\Omega}$. According to assumption (1) and Eq. (3.6), the resonance frequency can be approximated by $\omega_0=\Omega$. The second and third factors in the denominator of Eq. (3.9) don't change significantly across the bubble radius range, and can be approximated as constants with $R_{eq}=R_{0\Omega}$. Hence,

$$\beta_\Omega = \frac{\pi\rho_\Omega^2\left[3(\gamma+1)\Omega^2-\omega_1^2-\omega_2^2-\omega_1\omega_2\right]^2 P_1^2P_2^2 n(R_{0\Omega})}{\rho_1^2\rho_2^2\omega_1^4\omega_2^4\left[P_1^2\frac{Z_\Omega}{Z_1}+P_2^2\frac{Z_\Omega}{Z_2}\right]\left[\left(\frac{R_{01}^2}{R_{0\Omega}^2}-1\right)^2+\delta_1^2\right]\left[\left(\frac{R_{02}^2}{R_{0\Omega}^2}-1\right)^2+\delta_2^2\right]} \times$$

$$\int_{R_{0\Omega}-\varepsilon}^{R_{0\Omega}+\varepsilon} \frac{dR_{eq}}{R_{eq}^2\left[\left(\frac{R_{0\Omega}^2}{R_{eq}^2}-1\right)^2+\delta_\Omega^2\right]} \ . \quad (3.10)$$

To solve the above integral, consider the variable transformation

$$q = \frac{R_{0\Omega}}{R_{eq}} - 1 \; ; \qquad dq = -\frac{R_{0\Omega}}{R_{eq}^2}\, dR_{eq} \quad . \tag{3.11}$$

The integral in Eq. (3.10) is then given by

$$I = \int_{R_{0\Omega}-\varepsilon}^{R_{0\Omega}+\varepsilon} \frac{dR_{eq}}{R_{eq}^2\left[\left(\frac{R_{0\Omega}^2}{R_{eq}^2} - 1\right)^2 + \delta_\Omega^2\right]} = \int_{q1}^{q2} \frac{-dq}{R_{0\Omega}\left[\left((q)(q+2)\right)^2 + \delta_\Omega^2\right]} \quad , \tag{3.12}$$

where

$$q_1 = \frac{R_{0\Omega}}{(R_{0\Omega}-\varepsilon)} - 1, \qquad q_2 = \frac{R_{0\Omega}}{(R_{0\Omega}+\varepsilon)} - 1 \quad . \tag{3.13}$$

Since, according to assumption (1), the contribution to the integral is from a narrow range of bubble radii near $R_{eq}=R_{0\Omega}$, the variable q is always small. Hence the following approximation can be made:

$$(q(q+2))^2 \cong 4q^2 \quad . \tag{3.14}$$

Taking advantage of this approximation, the integral is

$$I = \frac{1}{R_{0\Omega}} \int_{-\infty}^{\infty} \frac{dq}{\left[4q^2 + \delta_\Omega^2\right]} \quad , \tag{3.15}$$

where the limits of integration have been expanded out to infinity. This is reasonable since the contribution to the integral is small outside the original limits q_1 and q_2. The resulting definite integral is tabulated:[24]

$$I = \frac{1}{R_{0\Omega}} \frac{\pi}{2\delta_\Omega} \quad . \tag{3.16}$$

Combine Eqs. (3.10), (3.12), and (3.16) to get an expression for β_Ω:

$$\beta_\Omega = \frac{\pi\rho_\Omega^2\left[3(\gamma+1)\Omega^2 - \omega_1^2 - \omega_2^2 - \omega_1\omega_2\right]^2 P_1^2 P_2^2 n(R_{0\Omega})}{\rho_1^2\rho_2^2\omega_1^4\omega_2^4\left[P_1^2\frac{Z_\Omega}{Z_1}+P_2^2\frac{Z_\Omega}{Z_2}\right]\left[\left(\frac{R_{01}^2}{R_{0\Omega}^2}-1\right)^2+\delta_1^2\right]\left[\left(\frac{R_{02}^2}{R_{0\Omega}^2}-1\right)^2+\delta_2^2\right]} \frac{1}{R_{0\Omega}} \frac{\pi}{2\delta_\Omega} \quad .(3.17)$$

β_1 and β_2 can be obtained by repeating the procedure of Eqs. (3.9) - (3.17) above, over bubble size ranges about R_{01} and R_{02}. The results are

$$\beta_1 = \frac{\pi\rho_\Omega^2\left[3(\gamma+1)\omega_1^2 - \omega_1^2 - \omega_2^2 - \omega_1\omega_2\right]^2 P_1^2 P_2^2 n(R_{01})}{\rho_1^2\rho_2^2\omega_1^4\omega_2^4\left[P_1^2\frac{Z_\Omega}{Z_1}+P_2^2\frac{Z_\Omega}{Z_2}\right]\left[\left(\frac{R_{0\Omega}^2}{R_{01}^2}-1\right)^2+\delta_\Omega^2\right]\left[\left(\frac{R_{02}^2}{R_{01}^2}-1\right)^2+\delta_2^2\right]} \frac{1}{R_{01}} \frac{\pi}{2\delta_1} \tag{3.18}$$

$$\beta_2 = \frac{\pi\rho_\Omega^2\left[3(\gamma+1)\omega_2^2 - \omega_1^2 - \omega_2^2 - \omega_1\omega_2\right]^2 P_1^2 P_2^2 n(R_{02})}{\rho_1^2\rho_2^2\omega_1^4\omega_2^4\left[P_1^2\frac{Z_\Omega}{Z_1}+P_2^2\frac{Z_\Omega}{Z_2}\right]\left[\left(\frac{R_{0\Omega}^2}{R_{02}^2}-1\right)^2+\delta_\Omega^2\right]\left[\left(\frac{R_{01}^2}{R_{02}^2}-1\right)^2+\delta_1^2\right]} \frac{1}{R_{02}} \frac{\pi}{2\delta_2} \quad .(3.19)$$

This page intentionally left blank.

4. DIFFERENCE FREQUENCY SCATTERING STRENGTH OF A GASSY SEAFLOOR

In Ref. 6 an expression was developed for the linear backscattering strength of a sediment interface, due to trapped bubbles within the volume below the interface. In this section, the same treatment will be followed in developing a difference frequency scattering strength.

In Section 4.1 an expression is derived for the scattered pressure from an element of sediment volume, based on the Biot theory and the principle of acoustic reciprocity. In Section 4.2, an expression is obtained for the effective scattering cross section per unit area of sediment interface.

4.1 SCATTERED PRESSURE FROM AN ELEMENT OF SEDIMENT VOLUME BY RECIPROCITY

Consider an acoustic source in the water column and an element of sediment volume that scatters sound, as in Fig. 4.1. The source and scatterer are both assumed to be much smaller than the acoustic wavelength. One can surround each with virtual spheres that are large in comparison with the wavelength, as in Fig. 4.2. The spheres surrounding source and scatterer will be called the "source sphere" and the "scatterer sphere", respectively.

The source sphere starts with a surface velocity v_0, which generates a pressure P at the scatterer. The scatterer sphere responds with a surface velocity v, which in turn induces a scattered pressure P_v back at the source. The pressures and surface velocities are related by the principle of acoustic reciprocity which states that, in a linear medium, the source and scatterer can be swapped with no change in the relationship between transmit and receive signals. For linear scattering problems this swapping of positions can be interpreted to represent the backscatter case. In terms of pressures and velocities, reciprocity states:

$$\frac{P}{v_0} = \frac{P_v}{v} \quad . \tag{4.1}$$

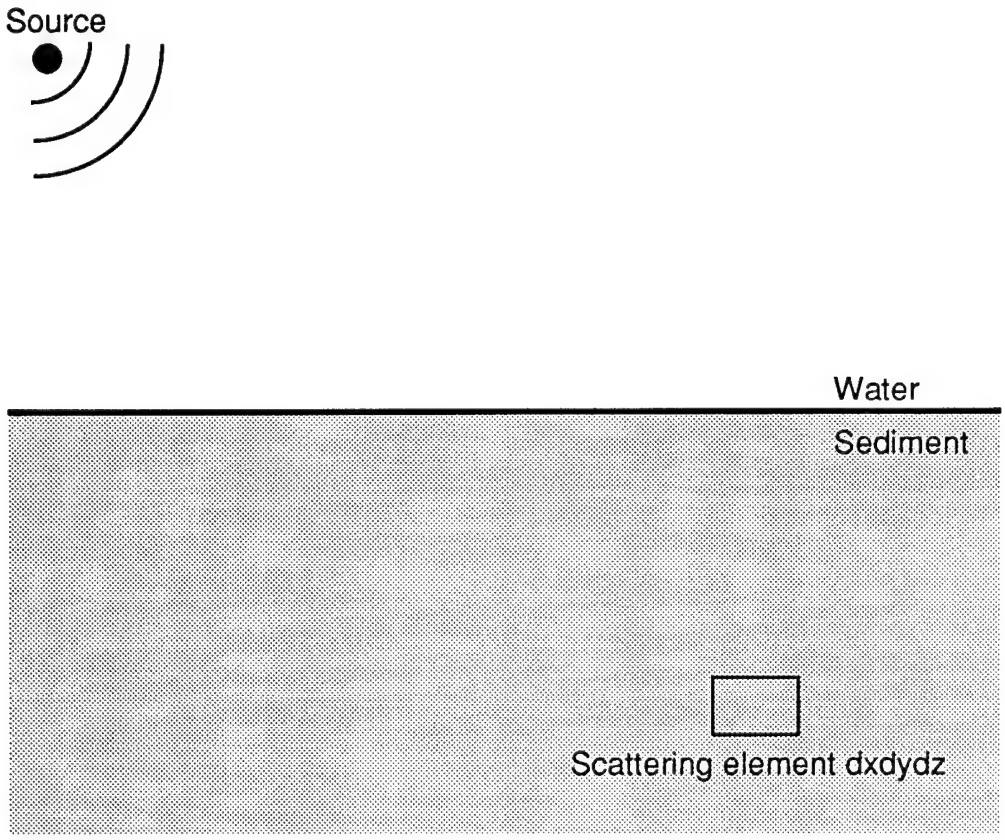

Figure 4.1
Backscatter from an element of sediment volume.

ARL:UT
AS-95-987
FAB - rfg
8-95

The surface velocities can be related to the local acoustic pressures and impedances:

$$v_0 = \frac{P_0}{Z_0} , \tag{4.2}$$

$$v = \frac{\varepsilon P}{Z} , \tag{4.3}$$

where Z_0 and Z are the acoustic impedances in the fluid above and in the sediment. ε is a transfer function from incident pressure P to scattered pressure εP at the surface of the scatterer sphere. It includes the combined effects of scattering at the element dxdydz and propagation from the scatterer to the surface of the surrounding virtual sphere. As illustrated in Fig. 4.2, this propagation takes place as if it were in the water column. If the water column's attenuation is neglected, the average square magnitude of ε is:

$$\langle |\varepsilon|^2 \rangle = \frac{\sigma_{bv} dxdydz}{4\pi r_s^2} , \tag{4.4}$$

where r_s is the radius of the virtual spheres and σ_{bv} is the scattering cross section, defined as the ratio of scattered power to incident intensity. By combining Eqs. (4.1) - (4.4), an expression is obtained for the square magnitude of the pressure returned to the projector:

$$\langle |P_v|^2 \rangle = \int \left| \frac{P}{P_0/Z_0} \right|^2 \frac{\sigma_{bv}}{4\pi r_s^2} |P/Z|^2 dxdydz . \tag{4.5}$$

Since the sediment under consideration is a Biot medium supporting fast and slow waves, the acoustic intensity returned to the projector has two components:

$$\langle |P_v|^2 \rangle = \int \left| \frac{P_f + P_s}{P_0/Z_0} \right|^2 \left(\frac{\sigma_{bvf}}{4\pi r_s^2} \left| \frac{P_f}{Z_f} \right|^2 + \frac{\sigma_{bvs}}{4\pi r_s^2} \left| \frac{P_s}{Z_s} \right|^2 \right) dxdydz , \tag{4.6}$$

where σ_{bvf} and σ_{bvs} are the scattering cross sections, per unit sediment volume, associated with the fast and slow waves. The quantities Z_f, Z_s, P_f, and P_s are,

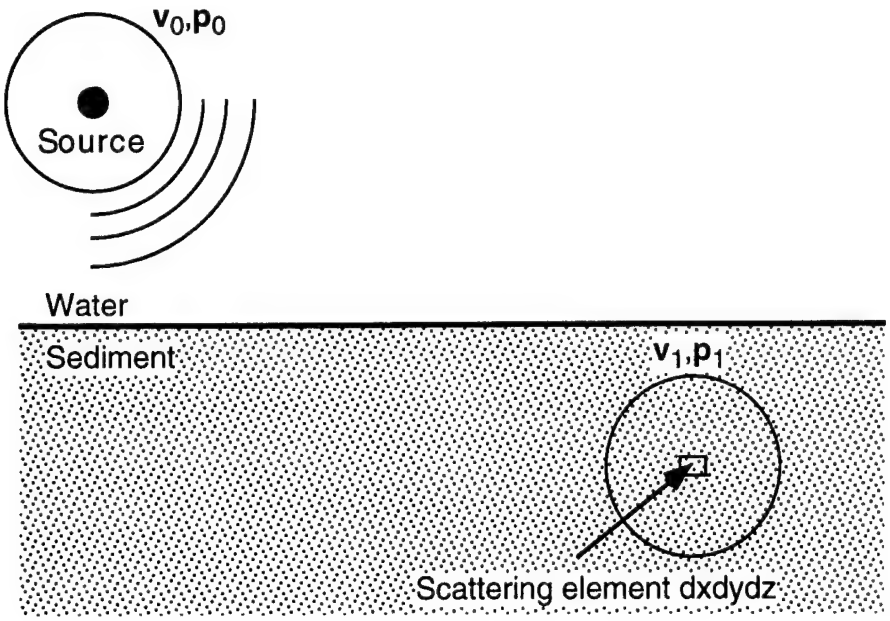

(a) Acoustic propagation of incident sound. Virtual sphere surrounding the source has surface velocity $\mathbf{v}_0$ and pressure $\mathbf{p}_0$. $\mathbf{v}_1$ and $\mathbf{p}_1$ are the pore fluid velocity and pressure induced at the scatterer.

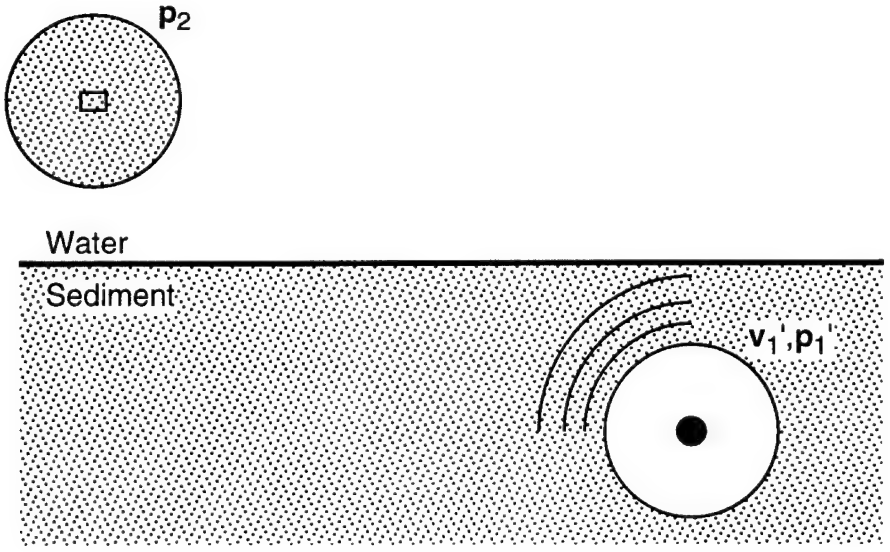

(b) Acoustic propagation of backscattered sound. Virtual sphere surrounding the scatterer has surface velocity $\mathbf{v}_1'$ and pressure $\mathbf{p}_1'$. $\mathbf{p}_2$ is the backscattered pressure induced at the source.

Figure 4.2
Calculation of backscatter by acoustic reciprocity.

ARL:UT
AS-95-988
FAB - rfg
8-95srvr

respectively, the fast and slow wave acoustic impedances and the acoustic pressures carried by the fast and slow wave. The quantity inside the parentheses is the square magnitude of the scatterer's surface velocity. The factor $\left|\frac{\mathbf{P_f+P_s}}{\mathbf{P_0/Z_0}}\right|^2$ converts this to the backscattered pressure magnitude squared.

Equation (4.6) involves linear scattering, where all propagation and scattering occurs at a single defined frequency. In the case of parametric scattering the incident sound upon the scatterer is at the primary frequencies, whereas the sound propagates away from the scatterer at the difference frequency. Care must be taken in specifying the frequencies at which the pressures and impedances in Eq. (4.6) are defined. The square magnitude of backscattered pressure at the difference frequency is

$$\langle |P_v|^2 \rangle = \int \zeta \left[\frac{\beta_f}{4\pi r_s^2} \left(\left| \frac{\mathbf{P_{1f}}}{\mathbf{Z_{1f}}} \right|^2 + \left| \frac{\mathbf{P_{2f}}}{\mathbf{Z_{2f}}} \right|^2 \right) + \frac{\beta_s}{4\pi r_s^2} \left(\left| \frac{\mathbf{P_{1s}}}{\mathbf{Z_{1s}}} \right|^2 + \left| \frac{\mathbf{P_{2s}}}{\mathbf{Z_{2s}}} \right|^2 \right) \right] dxdydz \quad , \quad (4.7)$$

where β_f and β_s are the difference frequency scattering cross sections, according to Eq. (4.1), for fast and slow waves, respectively. $\mathbf{P_{1f}}$, and $\mathbf{P_{2f}}$ are fast wave acoustic pressures incident upon the scattering element dxdydz at the primary frequencies ω_1 and ω_2. $\mathbf{P_{1s}}$ and $\mathbf{P_{2s}}$ are slow wave acoustic pressures incident upon the element. $\mathbf{Z_{1f}}$, $\mathbf{Z_{2f}}$, $\mathbf{Z_{1s}}$, and $\mathbf{Z_{2s}}$ are the corresponding partial acoustic impedances.

The quantity inside the brackets is the Ω component of the scattering sphere's surface velocity. The factor ζ converts this to the backscattered pressure returned to the projector. According to the principle of acoustic reciprocity, this is given by

$$\zeta = \left| \frac{\mathbf{P_{\Omega f}+P_{\Omega s}}}{\mathbf{P_{\Omega 0}/Z_{\Omega 0}}} \right|^2 , \quad (4.8)$$

where $\mathbf{P_{\Omega f}}$ and $\mathbf{P_{\Omega s}}$ are the fast and slow acoustic pressures that would be induced at frequency Ω upon the scattering element, if the fluid surrounding the source were driven at frequency Ω with velocity $\mathbf{P_{\Omega 0} / Z_{\Omega 0}}$.

4.2 DIFFERENCE FREQUENCY BACKSCATTERING STRENGTH OF SEDIMENT INTERFACE

In the following, the difference frequency backscattering strength of the sediment interface is defined. The definition is similar to that for linear scattering from bubbles.[25] As illustrated in Fig. 4.3, the effective surface backscattered pressure $\mathbf{P_s}$ per unit area dxdy of sediment interface is a sum of contributions from all volume scattering elements below the interface:

$$\langle |\mathbf{P_s}|^2 \rangle = \int_0^\infty \left| \frac{\mathbf{P_{\Omega f}+P_{\Omega s}}}{\mathbf{P_{\Omega 0}/Z_{\Omega 0}}} \right|^2 \left[\frac{\beta_f}{4\pi r_s^2} \left(\left| \frac{\mathbf{P_{1f}}}{\mathbf{Z_{1f}}} \right|^2 + \left| \frac{\mathbf{P_{2f}}}{\mathbf{Z_{2f}}} \right|^2 \right) + \frac{\beta_s}{4\pi r_s^2} \left(\left| \frac{\mathbf{P_{1s}}}{\mathbf{Z_{1s}}} \right|^2 + \left| \frac{\mathbf{P_{2s}}}{\mathbf{Z_{2s}}} \right|^2 \right) \right] dz \ . \quad (4.9)$$

The parametric backscattering strength is given in terms of the pressure $\mathbf{P_{inc}}$ incident upon an interface element dxdy and the scattered pressure $\mathbf{P_{s1}}$ at unit distance r_{1m} from dxdy:

$$|\mathbf{P_{s1}}| = |\mathbf{P_s}| \frac{r}{r_{1m}} e^{r\alpha} \ , \quad (4.10)$$

where r is the distance between the source in the water column and the scattering element dxdy, and α is the absorption in the water column. The backscattering strength of the interface is defined as

$$BS = 10 \log \frac{\langle |\mathbf{P_{s1}}|^2 \rangle}{|\mathbf{P_{inc}}|^2} \ . \quad (4.11)$$

Upon substituting Eqs. (4.9) and (4.10) into Eq. (4.11),

$$BS = 10 \log \frac{\left(\frac{r}{r_{1m}}\right)^2 e^{2r\alpha} \int_0^\infty \left| \frac{\mathbf{P_{\Omega f}+P_{\Omega s}}}{\mathbf{P_{\Omega 0}/Z_{\Omega 0}}} \right|^2 \left[\frac{\beta_f}{4\pi r_s^2} \left(\left| \frac{\mathbf{P_{1f}}}{\mathbf{Z_{1f}}} \right|^2 + \left| \frac{\mathbf{P_{2f}}}{\mathbf{Z_{2f}}} \right|^2 \right) + \frac{\beta_s}{4\pi r_s^2} \left(\left| \frac{\mathbf{P_{1s}}}{\mathbf{Z_{1s}}} \right|^2 + \left| \frac{\mathbf{P_{2s}}}{\mathbf{Z_{2s}}} \right|^2 \right) \right] dz}{|\mathbf{P_{inc}}|^2} \ . \quad (4.12)$$

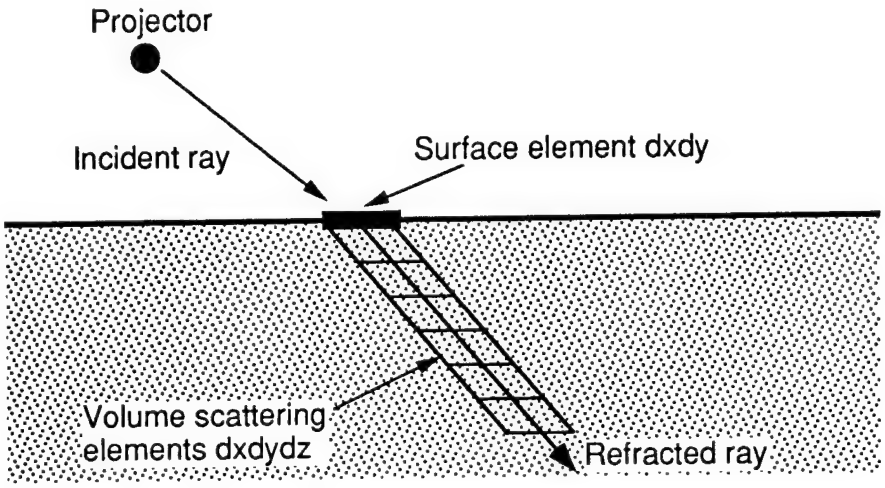

Figure 4.3
Effective interface backscatter due to volume scattering.

ARL:UT
AS-95-989
FAB - rfg
8-95

If the absorption in the water column is neglected,

$$BS = 10 \log \frac{\int_0^{\infty} \left| \frac{\mathbf{P}_{\Omega f}+\mathbf{P}_{\Omega s}}{\mathbf{P}_{\Omega i}/Z_{\Omega 0}} \right|^2 \left[\frac{\beta_f}{4\pi r_s^2} \left(\left| \frac{\mathbf{P}_{1f}}{Z_{1f}} \right|^2 + \left| \frac{\mathbf{P}_{2f}}{Z_{2f}} \right|^2 \right) + \frac{\beta_s}{4\pi r_s^2} \left(\left| \frac{\mathbf{P}_{1s}}{Z_{1s}} \right|^2 + \left| \frac{\mathbf{P}_{2s}}{Z_{2s}} \right|^2 \right) \right] dz}{|\mathbf{P}_{1i}+\mathbf{P}_{2i}|^2} \quad ,(4.13)$$

where $\mathbf{P}_{1i}$ and $\mathbf{P}_{2i}$ are the pressures of the incident sound at the primary frequencies ω_1 and ω_2. $\mathbf{P}_{\Omega i} = \mathbf{P}_{\Omega 0}(r_{1m}/r)$ is the incident acoustic pressure at the difference frequency Ω when $\mathbf{P}_{\Omega 0}$ is generated at the source sphere.

Figure 4.4(a) is a plot of the difference frequency backscattering strength modeled by Eq. (4.12) for a typical coarse sandy sediment. The sediment parameters are listed in Table 4.1. The backscattering strength in this figure increases with frequency. This is consistent with expectations, based on the bubble size density function, which was derived from the measured grain size distribution function. Over the frequency range of Fig. 4.4(a), the bubble size density function increases as the bubble radius decreases. Since the model is based on resonance scattering from bubbles, an increase in the scattering strength with frequency is expected.

The sediment parameters are listed in Table 4.1. The backscattering strength in this figure increases with frequency because of the bubble size density function, which decreases with bubble size. Since the model is based on resonance scattering from bubbles, this means that the backscattering strength should increase with frequency, which is consistent with the model's behavior.

In Fig. 4.4(b), the dependence of the backscattering strength on the incident primary pressure is plotted. The two primary pressures are assumed in this figure to have the same amplitude. The backscattering strength increases linearly with the primary signal pressure.

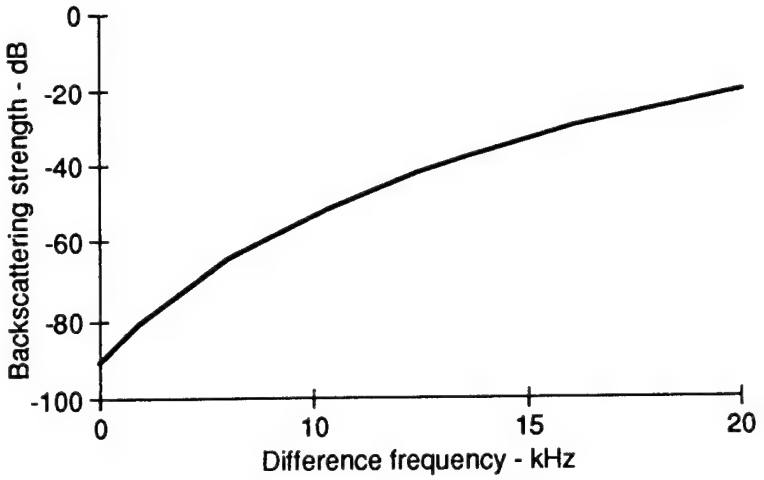

(a) Backscattering strength versus difference frequency for source level of 200 dB re 1 μPa and center frequency of 42 kHz, at normal incidence.

(b) Backscattering strength versus source level (at primary frequencies) for a difference frequency of 10 kHz and center frequency of 42 kHz, at normal incidence.

Figure 4.4
Predicted parametric backscattering strengths over a gassy sand with geoacoustic properties given in Table 4.1.

ARL:UT
AS-95-990
FAB - rfg
8-95

Table 4.1
Geoacoustic input parameters for parametric scattering strengths of Fig. 4.4.

Parameter	Units	
Fluid density	(kg/m^3)	1000
Fluid bulk modulus	(Pa)	2.25×10^9
Porosity		0.4
Grain density	(kg/m^3)	2650
Mean grain diameter	(ϕ)*	1.0
Standard deviation	(ϕ)*	1.0
Pore size parameter	(m)	1.796×10^{-4}
Viscosity	(kg/m-s)	1.0×10^{-3}
Permeability	(m^2)	6.45×10^{-10}
Virtual mass parameter		1.75
Grain bulk modulus	(Pa)	7.0×10^9
Frame shear modulus	(Pa)	2.61×10^7
Shear log decrement		0.15
Frame bulk modulus	(Pa)	5.3×10^9
Bulk log decrement		0.15
Gas bulk modulus	(Pa)	2.48×10^5
Gas density	(kg/m^3)	1.22
Gas heat conductivity	(cal/m-s-°C)	5.6×10^{-3}
Gas spec. heat (const press)	(cal/kg)	240
Gas specific heat ratio, C_p/C_v		1.4
Bubble surface tension	(N/m^2)	0.075
Bubble/pore volume ratio		0.625
Gas content		1.0×10^{-5}

* $\phi = -\log_2$(grain diameter in millimeters)

5. CONCLUSIONS

A model for parametric backscatter from trapped bubbles in sandy sediments has been developed. It is based on the nonlinear behavior of a gas bubble in an acoustic fluid, with modifications that allow the treatment of bubbles in a poroelastic medium. These modifications consist of assigning the pore fluid effective densities and acoustic impedances that characterize the Biot fast and slow waves.

The model's predictions are consistent with expectations. The backscattering strength increases linearly with source strength, which is identical to the case for parametric scattering from bubbles in an acoustic fluid. The increase in parametric backscattering strength with frequency is consistent with the bubble size distribution inferred from the input grain size distribution.

Similar parametric scattering models have been developed for bubbles in water,[26] and these compare reasonably well with experimental measurements. This work allows an application of this modeling technique to gas bubbles that might be trapped within sediment. At present, however, the authors are aware of no experimental measurements of parametric scattering strengths from sediments where the gas bubble size distributions are known. Such data are needed, when they become available, to test and further develop this model.

This page is intentionally left blank.

APPENDIX A

DERIVATION OF NONLINEAR EQUATION OF MOTION FOR A SINGLE BUBBLE

This page intentionally left blank.

The following derivation follows the treatments of Noltinigk and Nepiras[27] and Zabolotskaya and Soluyan.[28] Their papers consider the volume oscillations of a bubble surrounded by water and insonified with a parametric source.

Consider a bubble surrounded by water. We are interested in obtaining a relationship between the radial velocity of the bubble's surface and the applied pressure. Let the bubble have a radius R, which differs from its equilibrium radius R_0.

The kinetic energy of the liquid surrounding the bubble is

$$KE = \frac{\rho}{2}\int_R^\infty 4\pi r^2\left(\frac{dr}{dt}\right)^2 dr \quad . \tag{A.1}$$

In an incompressible medium, the radial velocity of the fluid surrounding the bubble would have a phase independent of the distance r from the bubble's center. The radial velocity dr/dt would then be given by

$$\frac{dr}{dt} = \frac{R^2}{r^2}\frac{dR}{dt} \quad . \tag{A.2}$$

In the case of a compressible medium, dr/dt will lag in phase behind dr/dt:

$$\frac{dr}{dt} = \frac{R^2}{r^2}\frac{dR}{dt}\, e^{-i\left(\frac{2\pi}{\lambda}\right)r} \quad , \tag{A.3}$$

where λ is the wavelength. Insert Eq. (A.3) into Eq. (A.1):

$$KE = \frac{\rho}{2}\int_R^\infty \frac{4\pi}{r^2}\left(R^2\frac{dR}{dt}\, e^{-i\left(\frac{2\pi}{\lambda}\right)r}\right)^2 dr$$

$$= 2\pi\rho\left(R^2\frac{dR}{dt}\right)^2\int_R^\infty \frac{e^{-2i\left(\frac{2\pi}{\lambda}\right)r}}{r^2}\, dr \quad . \tag{A.4}$$

When the bubble radius R is small in comparison with the wavelength λ, Eq. (A.4) can be approximated:

$$KE = 2\pi\rho\left(R^2\frac{dR}{dt}\right)^2\int_R^\infty \frac{dr}{r^2}$$

$$= 2\pi\rho R^3\left(\frac{dR}{dt}\right)^2 \quad . \tag{A.5}$$

This kinetic energy can be equated to the work done by the gas inside the bubble:

$$2\pi\rho R^3\left(\frac{dR}{dt}\right)^2 = \int_{V_0}^{V}(P_a - P)dV$$

$$= \int_{R_0}^{R}(P_a - P)(4\pi r^2)dr \quad , \tag{A.6}$$

where V_0 and R_0 are the bubble's equilibrium volume and radius. P_a is the pressure inside the bubble and P is the ambient pressure. Differentiating both sides with respect to R gives

$$2\pi\rho\left(3R^2\left(\frac{dR}{dt}\right)^2 + R^3\frac{d}{dR}\left(\frac{dR}{dt}\right)^2\right) = (P_a - P)(4\pi R^2) \quad . \tag{A.7}$$

Upon rearranging, the well known Rayleigh equation of motion is obtained:

$$R\frac{d^2R}{dt^2} + \frac{3}{2}\left(\frac{dR}{dt}\right)^2 = \frac{1}{\rho}(P_a - P) \quad , \tag{A.8}$$

where R is the bubble radius, ρ is the density of the surrounding fluid, P_a is the gas pressure inside the bubble, and P is the ambient pressure outside the bubble. In terms of the bubble volume $V = 4/3\,\pi R^3$, this equation can be rewritten:

$$aV^{-1/3}\ddot{V} - \frac{a}{6}V^{-4/3}\dot{V}^2 = P_a - P \quad , \tag{A.9}$$

where

$$a = \frac{\rho_0}{\sqrt[3]{3}}(4\pi)^{2/3} \quad . \tag{A.10}$$

Upon making the substitution $aV^{-1/3}=\rho_0/(4\pi R)$ and rearranging, Eq. (A.9) becomes

$$\ddot{V} - \frac{1}{6}\frac{\dot{V}^2}{V} - \frac{4\pi R}{\rho_0}P_a = -\frac{4\pi R}{\rho_0}P \quad . \tag{A.11}$$

If we assume that bubble oscillations are adiabatic, the relationship between bubble volume and internal pressure is given by

$$P_a = P_{eq}\left(\frac{V_{eq}}{V}\right)^{\gamma} \quad , \tag{A.12}$$

where γ is the ratio of specific heats. For small oscillations, the pressure, bubble radius, and volume can be expressed as equilibrium values with small perturbations:

$$P = P_{eq} + P' \tag{A.13}$$

$$R = R_{eq} + R' \tag{A.14}$$

$$V = V_{eq} + V' \quad . \tag{A.15}$$

The time derivative of V_{eq} is zero; therefore,

$$\dot{V} = \frac{d}{dt}V' \tag{A.16}$$

$$\ddot{V} = \frac{d^2}{dt^2}V' \quad . \tag{A.17}$$

Equation (A.12), for small perturbations, is therefore

$$P_a = P_{eq}\left(\frac{V_{eq}}{V_{eq}+V'}\right)^{\gamma} \quad . \tag{A.18}$$

To second order in (V'/V_{eq}), this is

$$P_a \cong P_{eq}\left(1-\gamma\frac{V'}{V_{eq}}+\frac{\gamma(\gamma+1)}{2}\left(\frac{V'}{V_{eq}}\right)^2\right) \quad . \tag{A.19}$$

Substituting Eq. (A.19) into Eq. (A.11),

$$\ddot{V}-\frac{1}{6}\frac{\dot{V}^2}{V}-\frac{4\pi R}{\rho_0}P_{eq}\left(-\gamma\frac{V'}{V_{eq}}+\frac{\gamma(\gamma+1)}{2}\left(\frac{V'}{V_{eq}}\right)^2\right)=\frac{4\pi R}{\rho_0}\left(P_{eq}-P\right) \quad . \tag{A.20}$$

Noting that the equilibrium volume is given by $V_{eq} = 4/3\pi R_{eq}^3$,

$$\ddot{V}-\frac{1}{6}\frac{\dot{V}^2}{V}+\frac{3\gamma R P_{eq}}{\rho_0 R_{eq}^3}V'-\frac{3\gamma R P_{eq}}{\rho_0 R_{eq}^3}\frac{3(\gamma+1)}{8\pi R_{eq}^3}V'^2=\frac{4\pi R}{\rho_0}\left(P_{eq}-P\right) \quad . \tag{A.21}$$

Upon making the following substitutions,

$$\omega_0^2=\frac{3\gamma P_{eq}}{\rho_0 R_{eq}^2} \tag{A.22}$$

$$\beta=\frac{1}{8\pi R_{eq}^3} \tag{A.23}$$

$$\varepsilon=\frac{4\pi R_{eq}}{\rho_0} \tag{A.24}$$

$$\alpha=3(\gamma+1)\omega_0^2\beta \ , \tag{A.25}$$

Eq. (A.21) can be written in the following form:

$$\ddot{V} - \frac{1}{6}\frac{\dot{V}^2}{V} + \frac{R}{R_{eq}}\omega_0^2 V' - \frac{R}{R_{eq}}\alpha V'^2 + \frac{R}{R_{eq}}\varepsilon P' = 0 \quad . \tag{A.26}$$

If we express R and V in terms of their equilibrium values and perturbations, Eq. (A.26) becomes

$$\ddot{V} - \frac{1}{6}\frac{\dot{V}^2}{V_{eq}}\left(\frac{V_{eq}}{V_{eq}+V'}\right) + \left(\frac{R_{eq}+R'}{R_{eq}}\right)\left(\omega_0^2 V' - \alpha V'^2 + \varepsilon P'\right) = 0 . \tag{A.27}$$

Expanding the quantities $\left(\frac{V_{eq}}{V_{eq}+V'}\right)$ and $\left(\frac{R_{eq}+R'}{R_{eq}}\right)$ to first order in V'/V_{eq},

$$\ddot{V} - \frac{1}{6}\frac{\dot{V}^2}{V_{eq}}\left(1 - V'/V_{eq}\right) + \left(1 + V'/3V_{eq}\right)\left(\omega_0^2 V' - \alpha V'^2 + \varepsilon P'\right) = 0 . \tag{A.28}$$

Upon rearranging, this expression can be written in the following form:

$$\ddot{V} - \frac{1}{6}\frac{\dot{V}^2}{V_{eq}} + \left(\omega_0^2 V' - \alpha V'^2 + \varepsilon P'\right) + \left(V'/V_{eq}\right)\left(\frac{1}{6}\frac{\dot{V}^2}{V_{eq}} + \frac{1}{3}\left(\omega_0^2 V' - \alpha V'^2 + \varepsilon P'\right)\right) = 0 . \tag{A.29}$$

Equation (A.26) can be rearranged as follows:

$$\omega_0^2 V' - \alpha V'^2 + \varepsilon P' = \frac{R_0}{R}\left(-\ddot{V} + \frac{1}{6}\frac{\dot{V}^2}{V}\right) \quad . \tag{A.30}$$

Expanding R_{eq}/R to first order in V'/V_{eq},

$$\omega_0^2 V' - \alpha V'^2 + \varepsilon P' = \left(1 - \frac{1}{3}\left(\frac{V'}{V_{eq}}\right)\right)\left(-\ddot{V} + \frac{1}{6}\frac{\dot{V}^2}{V}\right) \quad . \tag{A.31}$$

By applying Eq. (A.31) as a substitution in the last term in Eq. (A.29), the following expression is obtained

$$\ddot{V} - \frac{1}{6}\frac{\dot{V}^2}{V_{eq}} + \left(\omega_0^2 V' - \alpha V'^2 + \varepsilon P'\right) + \left(\frac{1}{6}\frac{\dot{V}^2}{V_{eq}}\frac{V'}{V_{eq}} + \frac{1}{3}\frac{V'}{V_{eq}}\left(-\ddot{V} + \frac{1}{6}\frac{\dot{V}^2}{V}\right)\left(1 - \frac{1}{3}\left(\frac{V'}{V_{eq}}\right)\right)\right) = 0 \tag{A.32}$$

By throwing out terms of order $(V'/V_{eq})^2$, Zabolotskaya's equation of motion for a bubble is obtained:

$$\ddot{V} - \frac{1}{6V_{eq}}\left(\dot{V}^2 + 2\ddot{V}V'\right) + \omega_0^2 V' - \alpha V'^2 = -\varepsilon P' \quad . \tag{A.33}$$

This expression neglects the possible loss of energy during bubble oscillation due to damping. In order to include damping, a term proportional to the time rate of change of bubble volume must be included, resulting in Zabolotskaya's damped equation of motion for the bubble:

$$\ddot{V} + \omega_0^2 V - \alpha V^2 - \beta\left(2\ddot{V}V + \dot{V}^2\right) + f\dot{V} = -\varepsilon P \quad . \tag{A.34}$$

The arbitrarily defined quantity f in Eq. (A.34) is related to the bubble's damping constant, δ[29-31] which is defined from the linear part of the bubble's equation of motion. If the nonlinear terms in Eq. (A.34) are neglected, the remaining equation is that of a damped harmonic oscillator,

$$\ddot{V} + f\dot{V} + \omega_0^2 V = -\varepsilon P, \tag{A.35}$$

with a damping constant given by

$$\delta = \frac{f}{\omega}, \tag{A.36}$$

where ω is the angular frequency. In terms of δ, the resulting equation of motion (A.34) is

$$\ddot{V} + \omega_0^2 V - \alpha V^2 - \beta\left(2\ddot{V}V + \dot{V}^2\right) + \omega\delta\dot{V} = -\varepsilon P \quad . \qquad \text{(A.37)}$$

In Zabolotskaya and Soloyan's treatment of bubbles in an acoustic fluid, the coefficients ω_0, α, β, and δ are invariant with respect to ω. More generally, as is the case for trapped bubbles in pores, these quantities must be allowed to vary with ω.

This page intentionally left blank.

APPENDIX B

RELATIONSHIP BETWEEN ACOUSTIC PRESSURE AND VOLUME OSCILLATION OF A MICROBUBBLE

This page intentionally left blank.

Equation (2.23) is a relationship between the pressures applied to a microbubble and the amplitude of its resulting volume variations. We are interested in the acoustic pressure radiated in the bubble's farfield. To that end we need a relationship between a bubble's volume oscillations and the acoustic pressure generated in the farfield. In developing such an expression, the following assumptions will be made.

(1) The bubble is small in relation to the acoustic wavelength.
(2) The signal amplitudes are small enough that the linear wave equation applies.

The linear wave equation in a fluid medium is given by

$$\nabla^2 \mathbf{p} = \frac{1}{c^2}\frac{\partial^2 \mathbf{p}}{\partial t^2} \quad , \tag{B.1}$$

where c is the phase velocity of a compressional wave in the fluid. For a pressure field that is spherically symmetric about a source at the origin, there is only radial dependence. The ∇^2 operator in this case is given by

$$\nabla^2 = \frac{\partial^2}{\partial r^2} + \frac{2}{r}\frac{\partial}{\partial r} \quad . \tag{B.2}$$

Upon substitution of Eq. (B.2) into (B.1) and rearranging, the wave equation can be written in the form

$$\frac{\partial^2 (r\mathbf{p})}{\partial r^2} = \frac{1}{c^2}\frac{\partial^2 (r\mathbf{p})}{\partial t^2} \quad . \tag{B.3}$$

General solutions for the quantity $r\mathbf{p}$ can be expressed as

$$r\mathbf{p} = f_1(ct-r) + f_2(ct+r) \quad , \tag{B.4}$$

where the first term represents a general incoming wave and the second term a general outgoing wave. If we consider outgoing harmonic waves only, the pressure field can be expressed as

$$\mathbf{p}(r) = \frac{\mathbf{A}}{r} \exp\left(i\left(\mathbf{k}r - \omega t\right)\right) \quad , \tag{B.5}$$

where **A** is an arbitrary complex amplitude, $\mathbf{k}=\omega/c+i\alpha$ is the acoustic wavenumber, α is the absorption in Np/m, and $\omega=2\pi f$ is the angular frequency. For small amplitude signals the fluid velocity is related to the acoustic pressure according to Euler's equation

$$\rho_0 \frac{\partial \vec{\mathbf{v}}}{\partial t} = -\nabla \mathbf{p} \quad , \tag{B.6}$$

where ρ_0 is the average density of the medium. Upon combination of Eqs. (A.5) and (A.6), a relation between acoustic pressure and fluid velocity is obtained:

$$\vec{\mathbf{v}}(r) = \hat{r}\left(1 - \frac{i}{\mathbf{k}r}\right)\frac{\mathbf{p}(r)}{\rho_0 c} \quad . \tag{B.7}$$

According to assumption (1), the quantity ka is small, where a is the bubble radius. Therefore the second term in Eq. (B.7) dominates at r=a:

$$\left|\mathbf{v}(a)\right| = \left|\frac{\mathbf{p}(a)}{\mathbf{k}a\rho_0 c}\right| \quad . \tag{B.8}$$

The acoustic pressure at r is inversely proportional to r:

$$\left|\mathbf{p}(r)\right| = \frac{a}{r}\left|\mathbf{p}(a)\right| \quad . \tag{B.9}$$

By combining Eqs. (B.8) and (B.9) and substituting $|\mathbf{k}|=\omega/c$,

$$\left|\mathbf{p}(r)\right| = \frac{\omega a^2 \rho_0 \left|\mathbf{v}(a)\right|}{r} \quad . \tag{B.10}$$

The rate of change of the bubble's volume perturbation V is related to its surface velocity **v**(a):

$$\frac{dV}{dt} = 4\pi a^2 \mathbf{v}(a). \tag{B.11}$$

If the oscillations are harmonic, the bubble volume rate dV/dt is related to its volume perturbation V:

$$\frac{dV}{dt} = \omega V , \tag{B.12}$$

where ω is the angular frequency. Upon combining Eqs. (B.10), (B.11), and (B.12),

$$|\mathbf{p}(r)| = \frac{\omega^2 \rho_0 |V|}{4\pi r} \quad . \tag{B.13}$$

This is Eq. (18) in Zabolotskaya and Sutin's paper,[33] originally derived by Landau and Lifshits.[34]

This page intentionally left blank.

REFERENCES

1. R. E. Patterson, "Backscatter of Sound from a Rough Boundary," J. Acoust. Soc. Am. 35, 2010-2013 (1963).

2. C. S. Clay and H. Medwin, *Acoustical Oceanography: Principles and Applications* (Wiley-Interscience, New York, 1977).

3. J. H. Stockhausen, "Scattering from the Volume of an Inhomogeneous Half-Space," NRE Report No. 63/9, Naval Research Establishment, Dartmouth, Nova Scotia, 1963.

4. D. R. Jackson, D. P. Winebrenner, and A. Ishimaru, "Application of the Composite Roughness Model to High-Frequency Bottom Backscattering," J. Acoust. Soc. Am. 79, 1410-1422 (1986).

5. P. C. Hines, "Theoretical Model of Acoustic Backscatter from a Smooth Seabed," J. Acoust. Soc. Am. 88, 324-334 (1990).

6. N. G. Pace, "Low Frequency Acoustic Backscatter from the Seabed," Proceedings, Institute of Acoustics 16(6), 181-188 (1994).

7. F. A. Boyle and N. P. Chotiros, "A Model for High Frequency Backscatter from Gas Bubbles in Sandy Sediments," J. Acoust. Soc. Am., accepted for publication, July 1995.

8. H. Medwin, "Counting Bubbles Acoustically, A Review," Ultrasonics 15(1) 7-13 (1977).

9. Ibid, Boyle and Chotiros.

10. J. M. Hovem, "The Nonlinearity Parameter of Saturated Marine Sediments," J. Acoust. Soc. Am. 66(5), 1463-1467 (1979).

11. V.G. Welsby and M. H. Safar, "Acoustic Non-Linearity due to Micro-Bubbles in Water," Acustica 22, 177-182 (1969/70).

12. T. G. Leighton, R. J. Lingard, A. J. Walton, and J. E. Field, "Acoustic Bubble Sizing by Combination of Subharmonic Emissions with Imaging Frequency," Ultrasonics 29, 319-323 (1991).

13. N. P. Chotiros and M. L. Ramaker, "High Frequency Acoustic Penetration of Sandy Ocean Sediments," presented at 121st Meeting of the Acoustical Society of America; J. Acoust. Soc. Am. 89(4), Pt. 2, 1908 (1991).

14. F. A. Boyle and N. P. Chotiros, "Experimental Detection of a Slow Acoustic Wave in Sediment at Shallow Grazing Angles," J. Acoust. Soc. Am. 91, 2615-2619 (1992).

15. M. A. Biot, "Theory of Propagation of Elastic Waves in a Fluid Saturated Porous Solid. I. Low Frequency Range," J. Acoust. Soc. Am. 28, 168-178 (1956).

16. M. A. Biot, "Theory of Propagation of Elastic Waves in a Fluid Saturated Porous Solid. II. Higher Frequency Range," J. Acoust. Soc. Am 28, 179-191 (1956).

17. M. Stern, A. Bedford, and H. R. Millwater, "Wave Reflection from a Sediment Layer with Depth-Dependent Properties," J. Acoust. Soc. Am. 77, 1781-1788 (1985).

18. L. A. Ostrovsky and A. M. Sutin, "Nonlinear Sound Scattering from Subsurface Bubble Layers," in *Natural Physical Sources of Underwater Sound*, B. R. Kerman, Ed. (Kluwer Academic Publishers, Dordrecht, Netherlands, 1993), 363-370.

19. E. A. Zabolotskaya and S. I. Soluyan, "Emission of Harmonic and Combination-Frequency Waves by Air Bubbles," Sov. Phys. Acoust. 18(3), 396-398 (1973), Eq. (7).

20. Ibid, Zabolotskaya and Soluyan, Eq. (17).

21. Ibid, Boyle and Chotiros (appendix).

22. R. Wildt, Ed., "Acoustic Theory of Bubbles," in *Physics of Sound in the Sea*, N.D.R.C. Summary Technical Report Div. 6, Vol. 8, Chap. 28, Washington, D.C. (1946).

23. Ibid, Medwin.

24. *Schaum's Outline Series: Mathematical Handbook of Formulas and Tables*, M. R. Speigel, Ed. (McGraw-Hill Book Co., Inc., New York, 1968).

25. Ibid, Boyle and Chotiros.

26. Ibid, Leighton et al.

27. B. E. Noltingk and E. A. Nepiras, "Cavitation Produced by Ultrasonics," Proc. R. Phys. Soc. London, Ser. B 63, 674-684 (1950).

28. E. A. Zabolotskaya and S. I. Soluyan, "Emission of Harmonic and Combination-Frequency Waves by Air Bubbles," Sov. Phys. Acoust. 18(3) 396-398 (1973).

29. Ibid, Medwin.

30. C. Devin, "Survey of Thermal, Radiation, and Viscous Damping of Pulsating Air Bubbles in Water," J. Acoust. Soc. Am. 31(12), 1654-1667 (1959).

31. Ibid, Wildt.

32. L. E. Kinsler, A. R. Frey, A. B. Coppens, and J. V. Sanders, *Fundamentals of Acoustics* (John Wiley and Sons, New York,1982), p.116.

33. E. A. Zabolotskaya and S. I. Sutin, "Emission of Harmonic and Combination-Frequency Waves by Air Bubbles," Sov. Phys. Acoust. 18(3) 396-398 (1973).

34. L. D. Landau and E. M. Lifshits, *Mechanics of Continuous Media* [in Russian] (GITTL, Moscow, 1953).

21 July 1995

DISTRIBUTION LIST
ARL-TR-95-19
Final Report under Subcontract 449382,
Applied Physics Laboratory, The University of Washington

Copy No.

Applied Physics Laboratory
The University of Washington
1013 NE 40th Street
Seattle WA 98105-6698

1 Attn: K. Williams

Commanding Officer
Naval Research Laboratory
Stennis Space Center, MS 39529-5004

2 Attn: R. Farwell (Code 7174)
3 D. Young (Code 7331)
4 P. Fleischer (Code 7430)
5 K. Briggs (Code 7430)
6 P. Valent (Code 7401)
7 R. Love (Code 7174)
8 B. Adams (Code 7180)
9 E. Franchi (Code 7105)
10 S. Stanic (Code 7174)
11 D. Ramsdale (Code 7170)
12 M. Richardson (Code 7430)
13 R. Meredith (Code 7172)
14 - 25 Library (Code 7035.3)

Office of Naval Research
Department of the Navy
Arlington, VA 22217-5000

26 Attn: J. Kravitz (Code 1125GG)
27 M. Badiey (Code 1125OA)
28 T. Simmen (Code 1125OA)
29 J. Beebe (Code 4433C)
30 E. Chaika (4431)
31 W. Ching (Code 4433)
32 T. Goldsberry (Code 4410)
33 D. Houser (Code 4424)

Distribution List for ARL-TR-95-19 under Subcontract 449382,
Applied Physics Laboratory, The University of Washington
(cont'd)

Copy No.

Commanding Officer
Naval Oceanographic Office
Stennis Space Center, MS 39522-5000
34 Attn: J. Bunce (OW)
35 E. Beeson (OARR)

Commander
Naval Oceanography Command
Stennis Space Center, MS 32522-5000
36 Attn: D. Durham (N5A)
37 R. L. Martin

Commander
Naval Sea Systems Command
Department of the Navy
Arlington, VA 22242-5160
38 Attn: J. Grembi (PMO407)
39 D. Gaarde (PMO407-2)

G & C Systems Manager
MK48/ADCAP Program Office
National Center 2
2521 Jefferson Davis Hwy.
12W32
Arlington, VA 22202
40 Attn: H. Grunin (PMO402E1)

Program Manager
MK50 Torpedo Program Office
Crystal Park 1
2011 Crystal Drive
Suite 1102
Arlington, VA 22202
41 Attn: T. Douglass (PMO406)

Commander
Dahlgren Division
Naval Surface Warfare Center
Dahlgren, VA 22448-5001
42 Attn: Library

Distribution List for ARL-TR-95-19 under Subcontract 449382,
Applied Physics Laboratory, The University of Washington
(cont'd)

Copy No.

Commander
Dahlgren Division
Naval Surface Warfare Center
Silver Spring, MD 20903-5000

43 Attn: S. Martin (U24)
44 J. Sherman (U20)
45 M. Stripling (U04)

Commanding Officer
Coastal Systems Station, Dahlgren Division
Naval Surface Warfare Center
Panama City, FL 32407-5000

46 Attn: M. Hauser
47 R. Johnson (Code 210T)
48 R. Lim
49 E. Linsenmeyer
50 D. Todoroff (Code 2120)

Commander
Naval Undersea Warfare Center Division
New London, CT 06320-5594

51 Attn: W. Roderick (Code 33A3)
52 J. Chester (Code 3331)
53 P. Koenig (Code 3331)

Commander
Naval Undersea Warfare Center Division
Newport, RI 02841-5047

54 Attn: J. Kelly (Code 3632)
55 F. Aidala (Code 362)
56 W. Gozdz (Code 36291)

Advanced Research Projects Agency
3701 North Fairfax Drive
Arlington, VA 22203-1714

57 Attn: W. Carey

Officer in Charge
Arctic Submarine Lab Detachment
Naval Undersea Warfare Center
San Diego, CA 92152-7210

58 Attn: R. Anderson (Code 19)

Distribution List for ARL-TR-95-19 under Subcontract 449382,
Applied Physics Laboratory, The University of Washington
(cont'd)

Copy No.

Chief of Naval Operations
Department of the Navy
Washington, DC 20360

59 Attn: R. Widmayer (OP 374T)
60 R. Winokur (OP 096T)
61 K. Martello (OP 954F1)
62 T. Fraim (OP 986G)
63 R. James (OP 006DX)
64 H. Montgomery (OP 9878)
65 J. Boosman (OP 987J)

Commander
Mine Warfare Command
Charleston Naval Base
Charleston, SC 29408

66 Attn: G. Pollitt (N3A)
67 B. O'Connel (N3A)

DTIC-OCC
Defense Technical Information Center
8725 John J. Kingman Road, Suite 0944
68 - 79 Fort Belvoir, VA 22060-6218

Applied Physics Laboratory
The University of Washington
1013 NE 40th Street
Seattle, WA 98105

80 Attn: D. Jackson
81 Library

Applied Research Laboratory
The Pennsylvania State University
P. O. Box 30
State College, PA 16804

82 Attn: R. Goodman
83 E. Liszka
84 Library
85 D. McCammon
86 S. McDaniel
87 F. Symons

Distribution List for ARL-TR-95-19 under Subcontract 449382,
Applied Physics Laboratory, The University of Washington
(cont'd)

Copy No.

	Presearch, Inc. 8500 Executive Park Avenue Fairfax, VA 22031
88 - 91	Attn: J. R. Blouin
	Physics Department The University of Texas at Austin Austin, TX 78712
92	Attn: W. D. McCormick
93	M. Fink
94	T. Griffy
	Aerospace Engineering Department The University of Texas at Austin Austin, TX 78712
95	Attn: M. Bedford
96	M. Stern
97	Robert A. Altenburg, ARL:UT
98	Hollis Boehme, ARL:UT
99	Frank A. Boyle, ARL:UT
100	Nicholas P. Chotiros, ARL:UT
101	John M. Huckabay, ARL:UT
102	Thomas G. Muir, ARL:UT
103	Library, ARL:UT
104 - 110	Reserve, ARL:UT